INTERNATIONAL INSTITUTE OF WELDING
A world of joining experience

XIII-2903-2021

FATIGUE STRENGTH AND RESIDUAL STRESS OF LONGITUDINAL ATTACHMENT JOINTS IMPROVED BY HFMI TREATMENT UNDER STATIC LOAD

Takeshi HANJI*, Kazuo TATEISHI, Suguru KANO and Masaru SHIMIZU
Nagoya University (Aichi, Japan, hanji@civil.nagoya-u.ac.jp)

ABSTRACT: In this study, the effect of the stress state of a welded joint during application of high-frequency mechanical impact (HFMI) treatment on the resulting fatigue strength was investigated through fatigue tests and finite element analysis. A high-frequency impact treatment tool was used as the HFMI device. Longitudinal attachment welded joints were treated under a state in which a static load was applied and subsequently tested under a constant stress amplitude with stress ratios of 0 or 0.5. The test results indicate that improved fatigue strength can be achieved even under a high stress ratio when the joint is treated under the minimum stress of fatigue loading. In addition, residual stress measurements and finite element analysis simulating welding and treatment processes indicated that the magnitude of compressive residual stress introduced to a weld toe is almost the same regardless of the stress state in the joint during treatment.

Keywords: high-frequency mechanical impact (HFMI) treatment, fatigue strength, residual stress, longitudinal attachment welded joints, treatment under static load

1. INTRODUCTION

Steel structures can develop fatigue cracks, and they usually occur at welded joints because the stress concentration is high and residual tensile stress is introduced by the welding process. To maintain and manage existing steel structures rationally and strategically, it is desirable to enhance the fatigue strength of welded joints, which may be critical from a fatigue point of view, as preventive maintenance.

A variety of post-weld treatment techniques are available for enhancing the fatigue strength of welded joints, and they are divided roughly into two types: weld geometry modification techniques and residual stress modification techniques [1]. The former can reduce the stress concentration by smoothing the weld geometry by burr-grinding and TIG dressing, while the latter can decrease the

*: corresponding author

Table 1 Mechanical properties and chemical composition of material in specimens

(a) Mechanical properties

Material	Yield stress (N/mm^2)	Tensile strength (N/mm^2)	Elongation (%)
Base metal (SBHS500)	587	679	30
Deposited metal	547	619	26

(b) Chemical compositions (mass%)

Material	C	Si	Mn	P	S	Cu	Ni	Cr	Mo	Nb	V
Base metal (SBHS500)	0.10	0.22	1.53	0.009	0.002	0.01	0.01	0.14	-	0.02	0.06
Deposited metal	0.05	0.53	1.45	0.009	0.005	0.27	0.51	0.02	0.01	-	0.01

Table 2 Welding conditions

Welding		Current	Voltage	Welding speed	Heat input
Step	Process	(A)	(V)	(cm/min)	(kJ/cm)
1	Full penetration welding	263.7	27.5	33.4	13.1
2	Boxing welding	240.7	27.7	33.6	11.9
3	Longitudinal fillet welding	247.6	27.6	35.3	11.6

tensile residual stress and, in many cases, introduce compressive residual stress around a weld toe. Hammer peening, needle peening [1], and high-frequency mechanical impact (HFMI) treatment [2] are among the techniques for residual stress modification. These methods also improve the weld toe geometry at the same time.

Fatigue strength improvement by HFMI treatment is known to depend on the stress ratio of fatigue loading, meaning that the fatigue strength benefits from HFMI treatment decrease as the stress ratio increases [3-10]. The IIW recommendations for HFMI treatment take this effect into account as an additional reduction in the number of FAT classes [2]. In particular, an increase in the stress ratio from 0.15 to 0.52 reduces the number of FAT classes to three, while no reduction can be considered when the stress ratio is less than 0.15. Therefore, if a structure is going to be subjected to a significant dead load when in use after HFMI treatment, it is necessary to take the stress ratio effect into account when assessing the fatigue strength of the treated joints.

Past study has shown the possibility that the fatigue strength of welded joints is enhanced remarkably, although the stress ratio is 0.5, when ultrasonic impact treatment is performed under a condition in which the maximum fatigue loading is statically applied [3]. This means that the stress ratio effect may depend on the stress state of a weld during the treatment. Further, it may not be necessary to consider the negative effect of the stress ratio on fatigue strength enhancement by HFMI treatment if it is performed when the structure is already in service, namely when a dead load is applied prior to treatment. Although this concept has been described in the IIW recommendation [2] and the AASHTO LRFD Bridge Construction Specifications [11], it can hardly be said that this point has been well verified so far.

In this study, HFMI treatment was applied to longitudinal attachment welded joints with different

stress states, and the effect on fatigue strength of the stress state of the joint during treatment was investigated through fatigue tests and finite element (FE) analysis.

2. EXPERIMENTAL PROCEDURE

2.1 Specimen Fabrication

Configurations and dimensions of the specimens are shown in Fig. 1. Longitudinal attachment welded joints were used for fatigue tests. The main plate and attachment were 12-mm thick, and the specimen width was 200 mm. The mechanical properties and chemical compositions of the steel and the deposited metal used in the specimens are listed in Table 1, which is from steel inspection certificates. Japan Industrial Standard (JIS) grade SBHS500, which is bridge high-performance steel, is a newly developed high-strength steel in Japan.

Carbon dioxide gas-shielded arc welding with a conventional wire 1.2 mm in diameter (JIS Z 3313 T59J1T1-1CA-N2M1-UH5) was used to fabricate the specimens. Table 2 gives the welding conditions. To avoid root fatigue cracking from a boxing weld between the main plate and the attachment, complete joint penetration welding was performed around the boxing weld, which was 50 mm from the attachment edge. In specimen fabrication, first, the attachment was fixed to the main plate with full penetration welding with a four-pass weld, and subsequently, boxing welding with a single-pass weld was performed to overlap the full penetration weld. Finally, the unwelded parts were connected with longitudinal fillet welding. Ultrasonic testing confirmed that no weld defects,

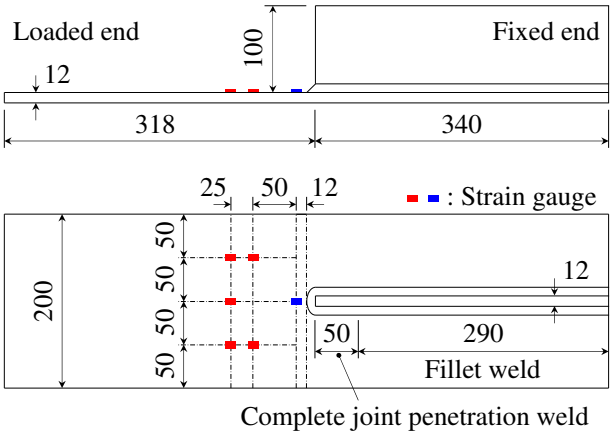

Fig. 1 Welding specimens (units: mm)

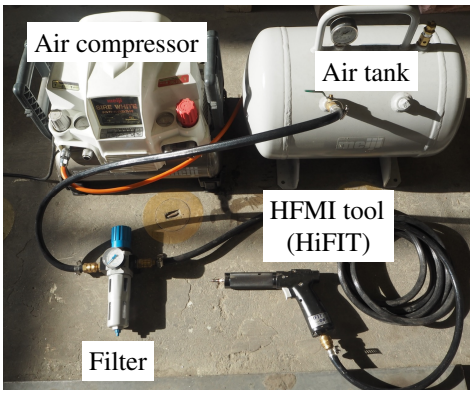

Fig. 3 HFMI treatment system

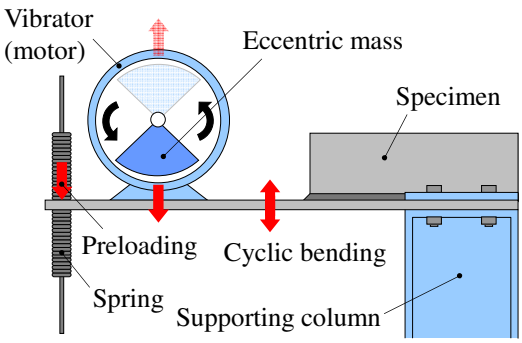

(a) Fatigue test

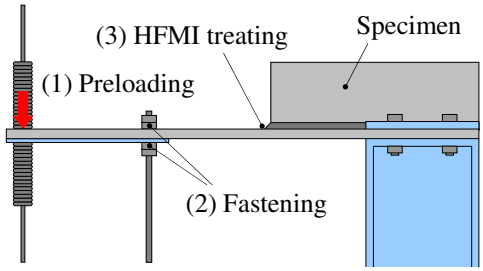

(b) HFMI treatment under static load

Fig. 2 Testing system

such as cracks and incomplete penetrations, existed in the boxing weld.

2.2 Loading Method

A fatigue testing system that can generate out-of-plane bending deformation in the main plate was used for the fatigue tests [12]. An overview of the testing system is shown in Fig. 2. One end of the main plate of the specimen was bolted to a supporting column and the other, unsupported end was subjected to cyclic loading by a vibration motor with an eccentric mass. Two stationary springs were affixed to the unsupported end of the specimen to induce a mean load in the specimen and change the stress ratio. The test was performed under a pulsating load with constant stress amplitude. The stress ratio at the weld was 0 or 0.5. The spring stiffness was set to maintain the mean stress during loading. The frequency of sinusoidal loading ranged from 9.9 to 15.5 Hz.

As shown in Fig. 1, strain gauges were placed on the main plate to monitor the stress range during the test. The nominal stress range for the specimen was determined by linearly interpolating the fluctuation ranges measured by the red gauges in Fig. 1 to the weld toe position. The number of cycles at which small cracks occurred along the weld toe was monitored by the blue gauge in Fig. 1. When the strain range monitored by this gauge dropped by 5% during the test, this was interpreted as the beginning of crack formation, and the corresponding number of cycles is denoted as $N_{5\%}$. The fatigue life of the specimen, denoted as N_{10}, was defined as the number of cycles at which a crack from the weld toe propagated 10 mm into the main plate. Enameled wires attached to the main plate surface, which would break due to cracking, were used to detect N_{10}. Cyclic loading was continued with an increased stress range when the specimen did not fail before 10 million cycles.

2.3 HFMI Treatment

The HFMI treatment system used in this study, which consisted of a HFMI tool, an air compressor, and an auxiliary air tank and filter element for dehumidification, is shown in Fig. 3. A pneumatic type HFMI device, specifically a high-frequency impact treatment (HiFIT) tool, was used for treatment. The diameter of the indenter was 3 mm. The compressed air pressure was monitored through a pressure indicator in the device and maintained at an almost constant 0.7 N/mm^2 during the treatment. The intensity of impact by the HiFIT tool could be changed by adjusting a setting dial on the back side of the tool; this intensity had a range of 0° to 960° (from lowest to highest). The impact frequency could be varied from 180 to 300 Hz depending on the intensity setting.

Specimens were treated under two stress levels. One level was treatment under no load, and the other was treatment under a static load applied to the specimen. The magnitude of the static load was

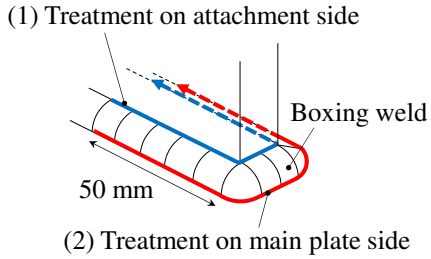

Fig. 4 HFMI treatment of boxing weld

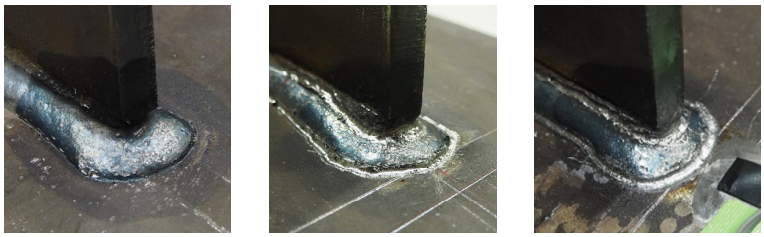

(a) As-welded toe (b) Treated toe under no load (c) Treated toe under static load

Fig. 5 Appearance of weld toes

Table 3 Measurement results of weld toe profile (upper row: mean; lower row: SD)

As-welded state		HFMI-treated state (under no load)				HFMI-treated state (under static load)			
Radius ρ_{aw} (mm)	Angle θ_{aw} (°)	Radius ρ_p (mm)	Angle θ_p (°)	Depth d (mm)	Width w (mm)	Radius ρ_p (mm)	Angle θ_p (°)	Depth d (mm)	Width w (mm)
0.73	50.2	2.15	36.6	0.37	2.41	2.34	35.8	0.38	2.57
0.23	3.96	0.41	4.94	0.09	0.26	0.19	2.39	0.03	0.16

set equal to the minimum load of the stress ratio of 0.5. The treatment under no load was performed by fixing four corners of the specimen before installing it in the testing system. As shown in Fig. 2(b), the static load was applied by adjusting the stationary springs, and after that, the specimen was fastened to the testing frame to hold the loading condition constant during treatment.

In this study, the boxing weld of the specimen was treated in three passes with an impact intensity of 180°. To prevent fatigue cracking from the weld toe on the attachment side, the weld toe on the attachment was treated prior to treatment of the weld toe on the main plate, as illustrated in Fig. 4. The treatment was performed according to the HiFIT instructions, but the working speed was a little slower than that given in the instructions to satisfy the HFMI groove profile recommended by IIW [2], which indicates an optimum HFMI groove 0.2–0.6 mm deep and 3–6 mm wide. The working speed for the weld toe on the main plate was approximately 1.4 mm/s. Photos of the boxing weld before and after the treatment are shown in Fig. 5. The appearance of the treated area was similar regardless of the loading condition during treatment.

3. EXPERIMENTAL RESULTS

3.1 Measurements of Weld Toe Profile

Weld toe profiles consisting of toe radius (ρ_{aw}) and weld angle (θ_{aw}) in the as-welded state, and toe radius (ρ_p), weld angle (θ_p), depth (d), and width (w) of the HFMI groove, as defined in Fig. 6, were measured for each specimen. The measurements were performed using a replica method. Silicon replicas of boxing weld beads were sliced, and then the profile of each sample was measured by image analysis.

The measurement results are summarized in Table 3, and the distributions between toe radius and weld angle and between groove width and depth are shown in Figs. 7 and 8, respectively. The toe radius became large and the toe angle became small compared to those in the as-welded state, meaning that the HFMI treatment forms the weld toe into a smooth profile. Moreover, it can be confirmed that most of the groove profiles are distributed to satisfy the IIW recommendations.

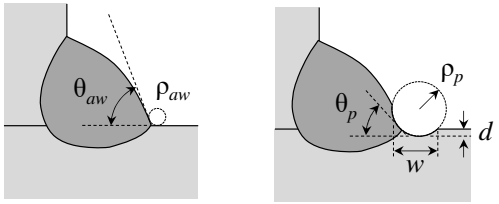

(a) As-welded state (b) Treated state

Fig. 6 Definition of weld toe profile

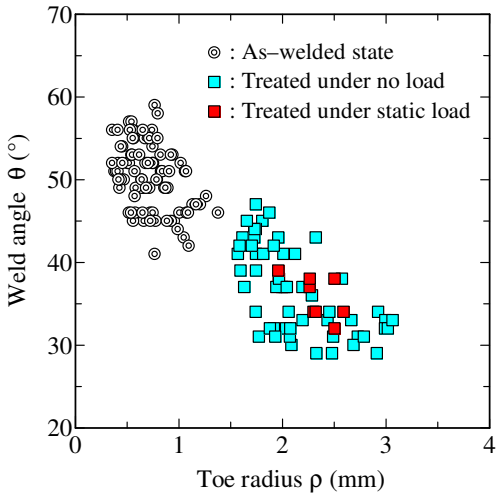

Fig. 7 Toe radius and weld angle

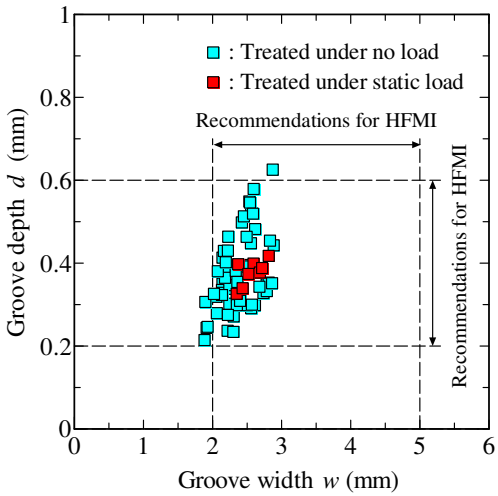

Fig. 8 HFMI groove profile

3.2 Residual Stress Measurements

Residual stress near the weld toe was measured by X-ray diffraction (μ-X360, PULSTEC) based on the cos α method. The direction of the residual stress in the specimen was longitudinal. The collimator size was 1 mm (2 mm on the illumination surface). After electropolishing of the specimen surface, the residual stresses were measured longitudinally at the middle width of the specimen starting from a point 2 mm away from the weld toe, as well as transversely 2 mm from the weld toe.

The measurements were performed before and after treatment. For the specimen treated under a static load, the load was applied to create a nominal stress of 200 N/mm^2 at the weld toe, and the residual stress after the treatment was measured while maintaining the load in the testing system. In this case, it was only possible to measure the residual stress 2 mm from the weld toe due to interference between the X-ray device and the testing system. The measurements for the other cases were performed before setting up the specimens in the testing system.

Figures 9 and 10 show the residual stress distribution in the longitudinal and transverse directions, respectively. The ordinates represent the residual stress, and the abscissas represent the longitudinal distance from the weld toe in Figs. 9(a) and 10(a) and the transverse distance from the center of the plate width in Figs. 9(b) and 10(b). In the graph, FE analysis results described in detail in Section 4 are also shown with broken lines for comparison.

In the as-welded state, a large tensile residual stress was introduced near the weld toe, and its magnitude decreased as the distance from the weld increased. Conversely, in the specimen treated under no load, a large compressive residual stress was introduced near the treated area, and the residual stress distribution tended to approach that in the as-welded state as the distance from the weld increased. Furthermore, similar residual stresses can be observed in both treated specimens, meaning that the HFMI treatment can sufficiently shift residual stress near the weld toe to the compression side regardless of the stress state of the joint during the treatment.

3.3 Fatigue Crack Observations

Figure 11 shows cracking patterns observed in the treated specimens. A fatigue crack grew from the treated area into the main plate in most specimens, while in some cases, a crack propagated from the weld toe on the attachment side.

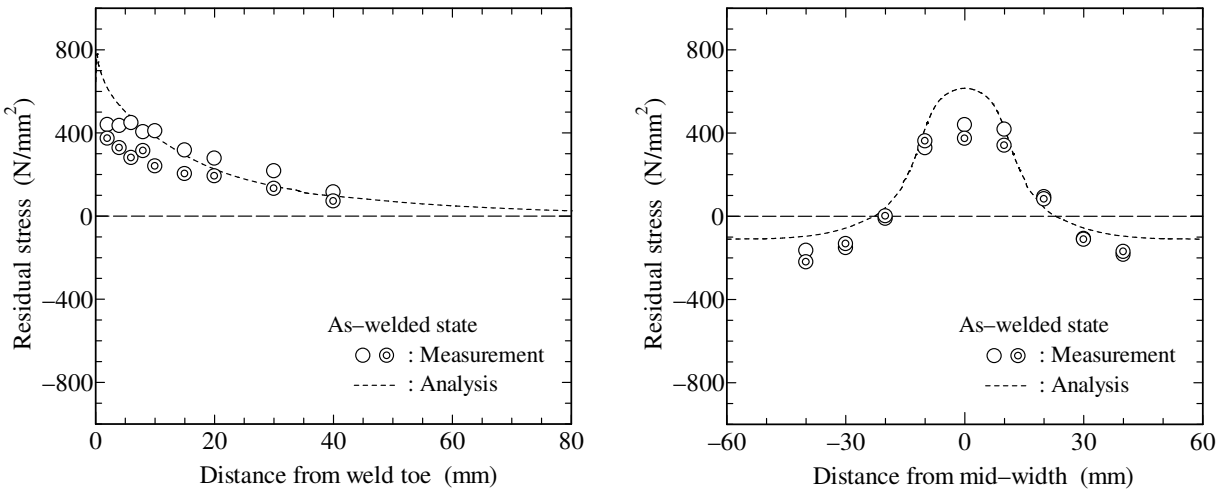

(a) Longitudinal direction (b) Transverse direction

Fig. 9 Residual stress distribution of the as-welded state

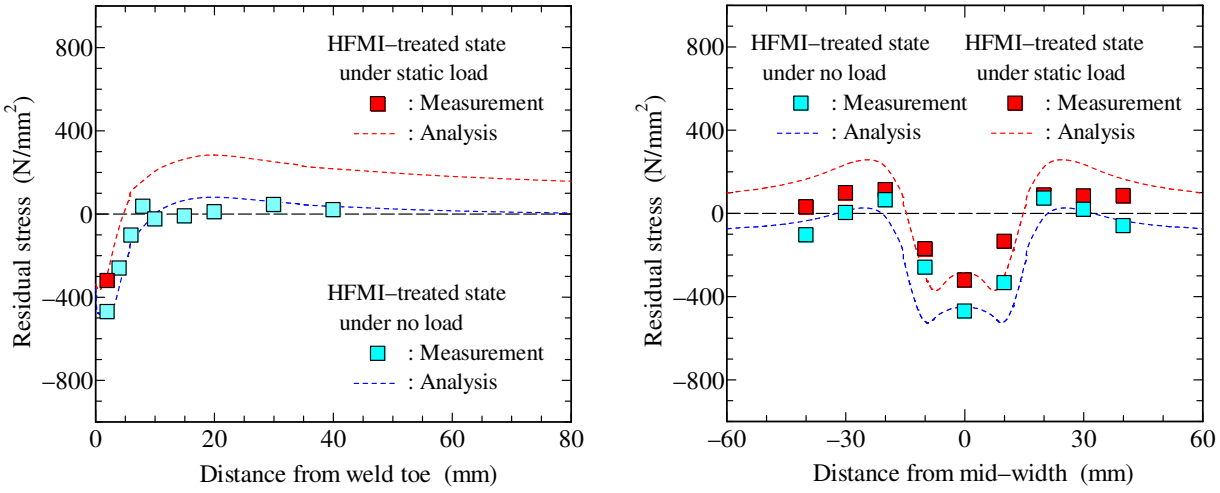

(a) Longitudinal direction (b) Transverse direction

Fig. 10 Residual stress distribution of HFMI-treated state

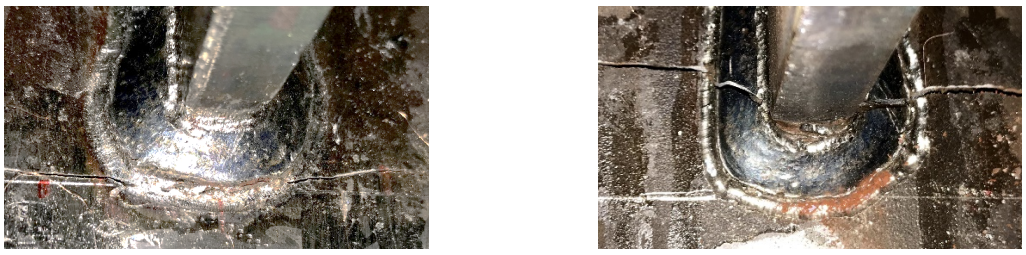

(a) Crack from HFMI groove on main plate (b) Crack from HFMI groove on attachment

Fig. 11 Cracking patterns in treated specimens

3.4 Fatigue Lives

Fatigue test results are summarized in Table 4 and shown in Figs. 12 and 13, together with the results in the as-welded state and as-treated states with different HFMI tools (see the caption of Fig. 12) obtained with the same type of joint and testing system [13, 14]. Here, the number of cycles required from the $N_{5\%}$ to N_{10} conditions is denoted as N_p. In the graphs, the fatigue strength curves

Table 4 Summary of fatigue tests in this study

No.	HFMI condition	Stress ratio	Stress range (N/mm^2)	$N_{5\%}$ ($\times 10^3$ cycles)	N_{10} ($\times 10^3$ cycles)	Notes
S1	no load	0	226.1	-	>10,000	Runout
S1R			270.5	-	>10,000	Retest of S1 with increased stress range Runout
S1R2			318.6	410	444	Retest of S1R with increased stress range
S2	no load	0	289.9	-	>10,000	Runout
S2R			323.3	620	652	Retest of S2 with increased stress range Crack from a toe on attachment side
S3	no load	0	343.1	40	63	Crack from a toe on attachment side
S4	no load	0.5	130.8	-	>10,000	Runout
S4R			152.3	-	>10,000	Retest of S4 with increased stress range Runout
S4R2			185.2	1,490	1,658	Retest of S4R with increased stress range
S5	no load	0.5	141.4	-	>10,000	Runout
S5R			165.5	580	740	Retest of S5 with increased stress range
S6	no load	0.5	202.3	40	63	
S7	under load	0.5	169.0	-	>10,000	Runout
S8	under load	0.5	199.4	-	>10,000	Runout

for the as-welded state specified by the Japanese Society of Steel Construction (JSSC) [15] are also shown. The values in parentheses represent the fatigue strength required at 2 million cycles for each category. In the graphs, specimens that failed by cracking from the attachment side are marked with an asterisk and specimens that did not fail before 10 million cycles are marked with an arrow.

When a stress ratio is 0, the fatigue strength of the specimen can be significantly enhanced by HiFIT, and the extent of the enhancement tends to be equal to or slightly higher than that of the other HFMI tools. In addition, the HFMI treatment seems to have a beneficial effect on the crack initiation stage rather than the crack propagation stage.

In the specimens treated under no load, fatigue strength enhancement under a stress ratio of 0.5 tended to decrease compared with those under a stress ratio of 0. In contrast, specimens treated under a static load did not fail even at a high stress range of 200 N/mm^2 with a stress ratio of 0.5, indicating that the fatigue strength may be close to that under a stress ratio of 0. These results, therefore, suggest that significant fatigue strength enhancement is achieved even under a high stress ratio when the HFMI treatment is applied to welded joints subjected to a dead load.

4. RESIDUAL STRESS SIMULATION BY FINITE ELEMENT ANALYSIS

Elasto-plastic FE analysis with simple consideration of welding and HFMI treatment was carried out to clarify the residual stress distributions around a weld due to the difference in stress states in the welded joint during treatment.

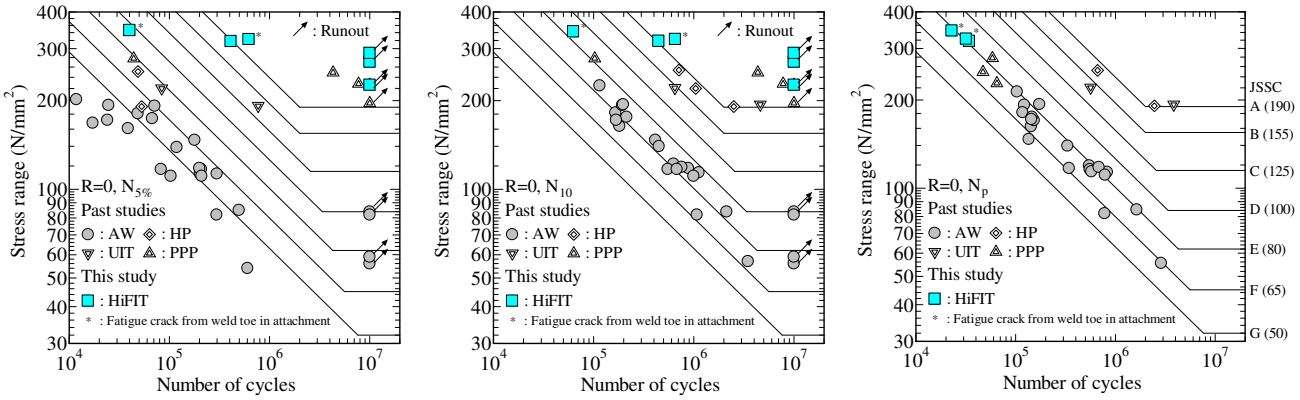

(a) $N_{5\%}$ (b) N_{10} (c) N_p

Fig. 12 Fatigue test results under a stress ratio of 0 (key to abbreviations: AW, as-welded; HP, hammer peening; UIT, ultrasonic impact treatment; PPP, portable pneumatic needle-peening)

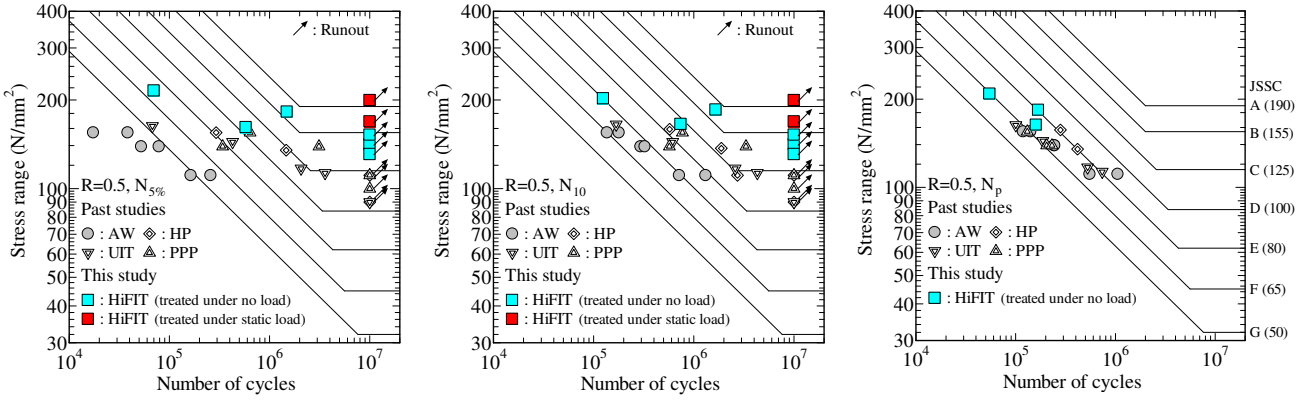

(a) $N_{5\%}$ (b) N_{10} (c) N_p

Fig. 13 Fatigue test results under a stress ratio of 0.5

4.1 Welding Simulation

Abaqus ver. 6.14 was used for the simulation with the FE model shown in Fig. 14. To reduce the calculation time of the simulation, a half model created with solid elements was used. Displacement constraints were applied to the main plate corners to avoid rigid-body motion of the model.

Welding simulation was performed using the element birth and death technique. In this method, weld-line elements are deactivated in the initial state and then reactivated and heated sequentially during the welding process. As shown in Fig. 15, the welding process was simply divided into three steps: (1) full penetration welding, (2) boxing welding, and (3) longitudinal fillet welding. All weld-line elements contained in each step were simultaneously activated and heated step by step, and then finally the model was cooled to room temperature. Heat input at each step was based on the specimen welding conditions. Thermal efficiency was set to be 80%. As shown in Fig. 16, the temperature dependence of material properties in the specimen was determined based on a past study [16].

Temperature histories obtained in the analysis are compared with those measured during specimen fabrication in Fig. 17. Temperature measurements were performed at four points on the specimen surface. Although full penetration welding was performed with multi-pass welds in the actual fabrication, this was simulated with a single pass in the analysis. Thus, the start time of the simulation was shifted to match the peak positions in the temperature histories of the measurement

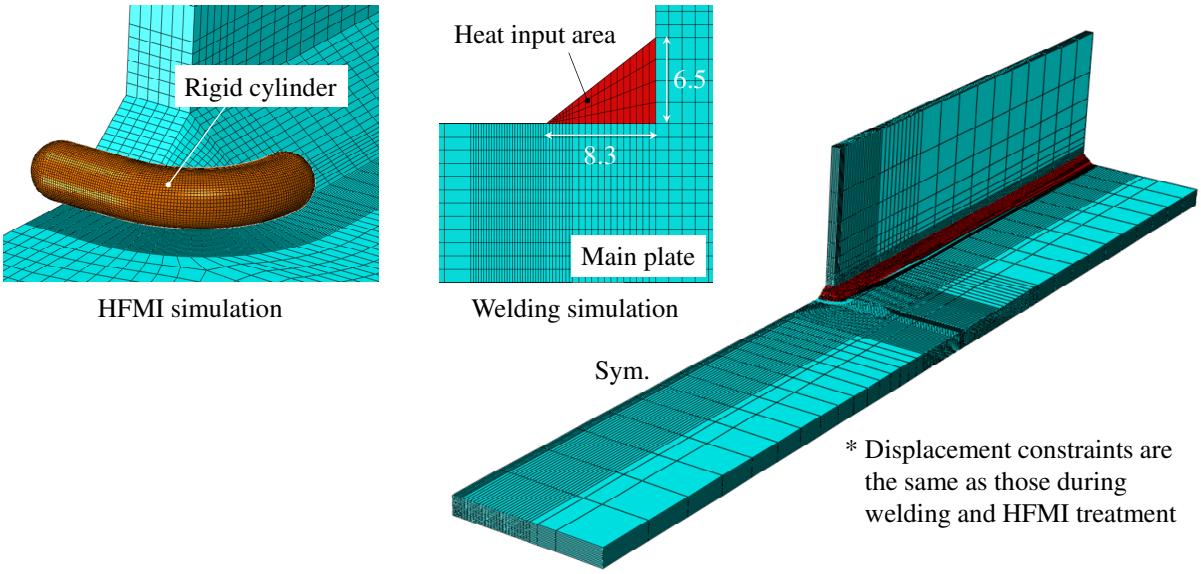

Fig. 14 FE model (unit: mm)

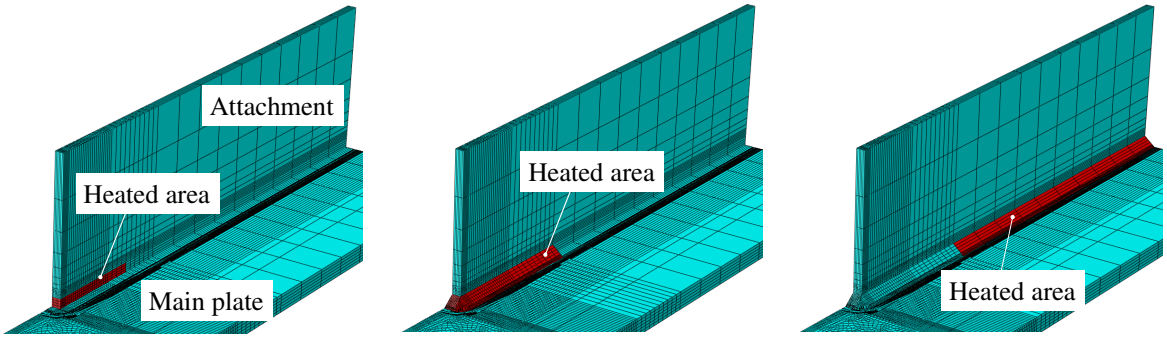

(a) Step 1 (b) Step 2 (c) Step 3

Fig. 15 Welding process in simulation

and the simulation. It can be confirmed that the analysis results correspond well with the measurements.

Figure 9 compares the welding residual stress distributions from the FE analysis and measurements using the X-ray diffraction method. The distributions are in relatively good agreement, indicating the validity of the FE models for the welding simulation.

4.2 Simulation of HFMI Treatment under No Load

A simulation of no-load HFMI treatment was performed on a model in which the residual stress distribution obtained by the welding simulation in Section 4.1 was given as the initial state. The boundary conditions were same as the conditions under which the specimens were treated.

The yield function f given in the following equations, which denotes the combined hardening rules [17, 18], was employed for the base metal as in past studies [19-21]:

$$f = \left|\sigma - X\right| - R - \sigma_y, \tag{1a}$$

$$R = R_\infty \left[1 - \exp\left(-b \cdot \varepsilon_p\right)\right], \tag{1b}$$

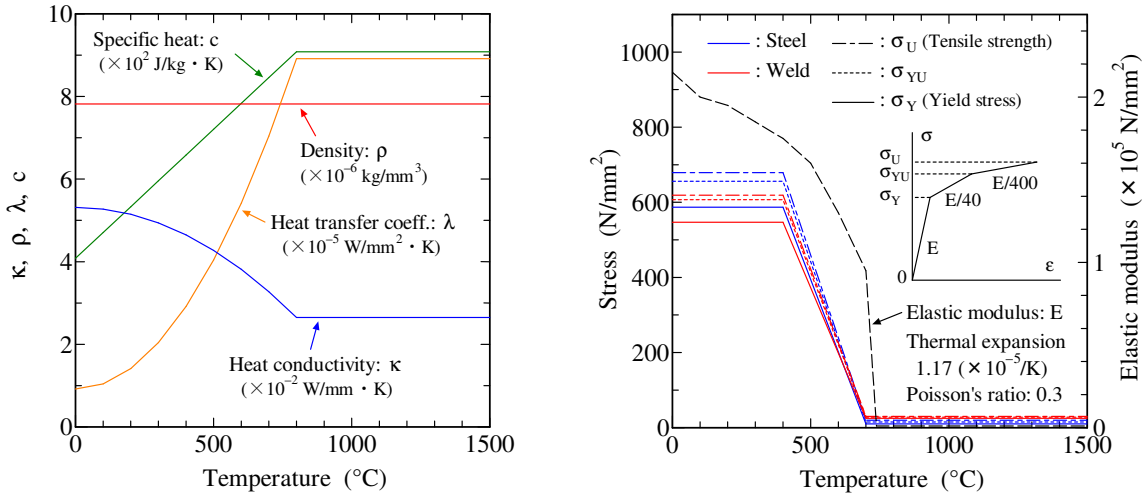

(a) Physical constants (b) Mechanical properties

Fig. 16 Temperature dependency of material properties in the FE model

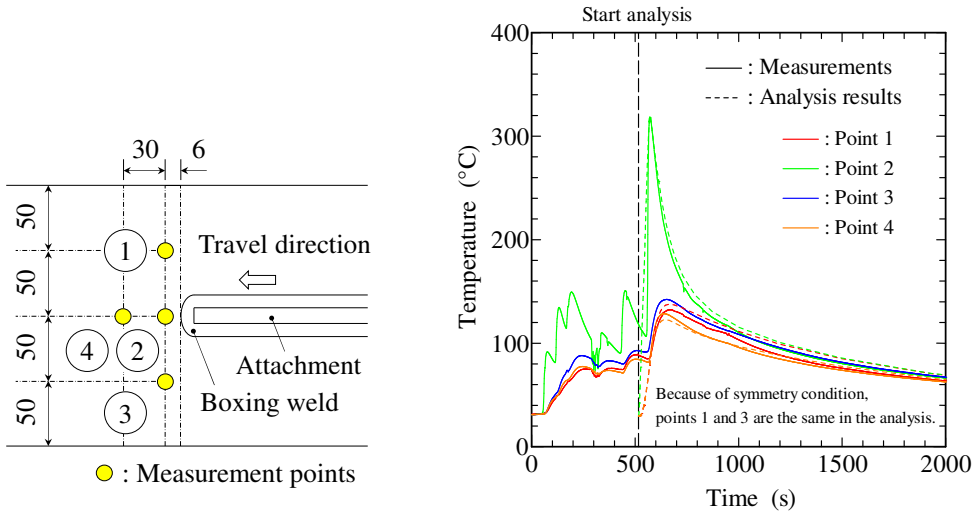

(a) Measurement points (unit: mm) (b) Comparisons of temperature histories

Fig. 17 Temperature histories

$$X = X_{\infty}\left[1-\exp\left(-\gamma\cdot\varepsilon_{p}\right)\right], \tag{1c}$$

where R is the isotropic hardening, X is the back stress, σ_y is the initial yield surface, σ is the subsequent yield surface, R_∞ and b are the material parameters for the isotropic hardening exponential law, X_∞ and γ are the nonlinear kinematic hardening parameters, and ε_p is the plastic strain.

Based on a tensile curve for repeated unloadings until compressive yield stress is reached [18], both isotropic and kinematic hardening parameters were identified for the base metal. The material test was performed using a round-bar specimen cut out from the same steel plate as the specimen, and its material parameters are listed in Table 5. Based on the material test, the elastic modulus and Poisson's ratio for the base metal were 213 kN/mm^2 and 0.3, respectively. In contrast, the deposited metal was assumed to follow a bilinear constitutive law based on the steel inspection certificate, with a secondary slope of the elastic modulus of 1/100, and the kinematic hardening model. An elastic

Table 5 Material parameters for combined hardening models

Material	σ_y (N/mm^2)	Isotropic hardening		Kinematic hardening	
		R_∞ (N/mm^2)	b	X_∞ (N/mm^2)	γ
Base metal (SBHS500)	512	135	2	174	82

modulus of 200 kN/mm^2 and Poisson's ratio of 0.3 were applied to the deposited metal.

In this analysis, a cylinder with a rigid body was set as shown in Fig. 14. The treatment process along the weld toe was simply simulated by statically pushing and pulling out a rigid body matching the actual groove radius and depth in the specimen.

Figure 10 shows the comparison of residual stresses introduced by the HFMI treatment in the analysis and the measurements. Relatively good agreement can be observed between them, meaning that even with a simple simulation of HFMI treatment of a weld toe, the residual stress distribution after the treatment can be obtained with sufficient accuracy.

4.3 Simulation of HFMI Treatment under a Static Load

A simulation of HFMI treatment was performed while applying a static load to a model given the residual stress distribution by the welding simulation as the initial state. The boundary conditions were the same as the conditions under which the specimen was installed in the testing system, and the static load was applied to the end of the main plate by vertical displacement. The magnitude of the displacement was determined to produce a nominal stress of 200 N/mm^2 at the weld toe, and it was confirmed that the stress distribution on the main plate surface due to this static load agrees well with the measurements by strain gauges. This treatment simulation was performed while applying a static load.

In the comparison of the residual stresses between the simulation and the measurements shown in Fig. 10, it can be confirmed that the residual stress obtained by the simulation tends to be similar to that actually measured in the specimen. Particularly in the vicinity of the treated area, the compressive residual stresses introduced by the treatment are almost the same regardless of the stress state of the weld during treatment. This result is consistent with the fact that in the fatigue test with a stress ratio of 0.5, and higher enhancement of fatigue strength was achieved when the treatment was performed under a static load compared to that under no load.

4.4 Residual Stress Distributions in the Thickness Direction

Figure 18 shows the residual stress distribution in the thickness direction obtained by the welding simulation and the HFMI treatment simulation with and without static loading. The ordinate represents the distance from the specimen surface at the weld toe position. The analysis result when a tensile load was applied as a static load instead of the bending load is also shown in the graph. The nominal stress at the weld toe in both cases was 200 N/mm^2.

In the case of treatment under no load, the result indicates that the treatment produced compressive residual stresses up to a depth of approximately 2–3 mm, which is similar to the residual stress distributions measured or analyzed in steel plates and welded joints treated by HFMI [19-22]. Furthermore, the tendency of residual stress distribution is nearly the same regardless of the stress states in the joint during treatment, suggesting that a beneficial compressive residual stress can

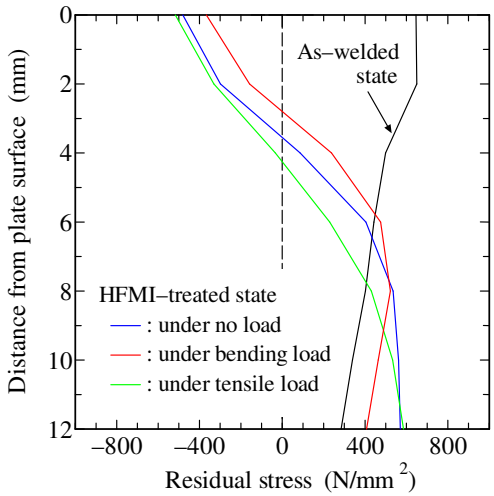

Fig. 18 Residual stress distributions in the thickness direction

be introduced to a depth of 2–3 mm even during treatment with a static load.

5. CONCLUSIONS

In this study, the effect of HFMI treatment under a static load, as a possible preventive maintenance method for existing structures, was investigated through fatigue tests with longitudinal attachment welded joints. In addition, FE analysis simulating welding and treatment processes was performed to confirm the residual stress distribution introduced by the treatment. The results obtained in this study are summarized as follows:

- The fatigue strength of a specimen can be significantly enhanced by HFMI treatment, and the extent of the enhancement tends to be almost the same regardless of the HFMI tool.
- The HFMI treatment seems to have a beneficial effect on the crack initiation stage rather than the crack propagation stage.
- The analysis results show that HFMI treatment imparts a beneficial compressive residual stress that reaches a depth of approximately 2–3 mm.
- The tendency of residual stress distribution is not significantly different regardless of the stress state in the joint during treatment, supporting the idea that HFMI treatment enhances fatigue strength of welded joints in existing structures.

ACKNOWLEDGMENTS

The authors gratefully acknowledge the support of the Japan Iron and Steel Federation and also express their sincere gratitude to Mr. Yoshimine at Nippon Sharyo, Ltd., for fabricating the specimens. In addition, the authors wish to thank Mr. Neher at HiFIT Vertriebs GmbH for his kind support of the HiFIT tool.

REFERENCES

[1] P.J. Haagensen and S.J. Maddox: IIW recommendations on methods for improving the fatigue strength of welded joints, *Woodhead Publishing*, 2013.

[2] G.B. Marquis and Z. Barsoum: IIW recommendations for the HFMI treatment for improving the fatigue strength of welded joints, *Springer*, 2016.

[3] T. Mori, H. Shimanuki and M. Tanaka: Effect of UIT on fatigue strength of web-gusset welded joints considering service condition of steel structures, *Welding in the World*, Vol.56, pp.141-149, 2012.
[4] T. Okawa, H. Shimanuki, Y. Funatsu, T. Nose and Y. Sumi: Effect of preload and stress ratio on fatigue strength of welded joints improved by ultrasonic impact treatment, *Welding in the World*, Vol.57, pp.235-241, 2013.
[5] G.B. Marquis, E. Mikkola, H.C. Yildirim and Z. Barsoum: Fatigue strength improvement of steel structures by high-frequency mechanical impact: proposed fatigue assessment guidelines, *Welding in the World*, Vol.57, pp.803-822, 2013.
[6] H. Shimanuki and T. Okawa: Effect of stress ratio on the enhancement of fatigue strength in high performance steel welded joints by ultrasonic impact treatment, *International Journal of Steel Structures*, Vol.13, pp.155-161, 2013.
[7] E. Mikkola, M. Doré G.B. Marquis and M. Khurshid: Fatigue assessment of high-frequency mechanical impact (HFMI)-treated welded joints subjected to high mean stresses and spectrum loading, *Fatigue & Fracture of Engineering Materials & Structures*, Vol.38, pp. 1167-1180, 2015.
[8] M. Leitner and M. Stoschka: Effect of load stress ratio on nominal and effective notch fatigue strength assessment of HFMI-treated high-strength steel cover plates, *International Journal of Fatigue*, Vol.139, 105784, 2020.
[9] T. Yonezawa, H. Shimanuki and T. Mori: Influence of cyclic loading on the relaxation behavior of compressive residual stress induced by UIT, *Welding in the World*, Vol.64, pp.171-178, 2020.
[10] M. Leitner and Z. Barsoum: Effect of increased yield strength, R-ratio, and plate thickness on the fatigue resistance of high-frequency mechanical impact (HFMI)-treated steel joints, *Welding in the World*, Vol.64, pp.1245-1259, 2020.
[11] American Association of State Highway and Transportation Officials: AASHTO LRFD bridge construction specifications, 3rd edition, 2010.
[12] K. Yamada, S. Ya, B. Baik, A. Torii, T. Ojio and S. Yamada: Development of a new fatigue testing machine and some fatigue tests for plate bending, *IIW documentation*, XIII-2161-07, 2007.
[13] Japanese Society of Steel Construction: JSSC Technical Report No.115, 2018 (in Japanese).
[14] Japanese Society of Steel Construction: JSSC Technical Report No.120, 2020 (in Japanese).
[15] Japanese Society of Steel Construction: Fatigue design recommendations for steel structures, 2012 (in Japanese).
[16] Y.C. Kim, J.Y. Lee and K. Inose: The high accurate prediction of welding distortion generated by fillet welding, *Quarterly Journal of the Japan Welding Society*, Vol.23, No.3, pp.431-435, 2005 (in Japanese).
[17] J. Lemaite and J. Chaboche: Mechanics of solid materials, *Cambridge University Press*, 1990.
[18] J. Lemaitre and R. Desmorat: Engineering damage mechanics, *Springer*, 2005.
[19] J. Foehrenbach, V. Hardenacke and M. Farajian: High frequency mechanical impact treatment (HFMI) for the fatigue improvement: numerical and experimental investigations to describe the condition in the surface layer, *Welding in the World*, Vol.60, pp.749-755, 2016.
[20] M. Leitner, M. Khurshid and Z. Barsoum: Stability of high-frequency mechanical impact (HFMI) post-treatment induced residual stress states under cyclic loading of welded steel joints, *Engineering Structures*, Vol.143, pp.589-602, 2017.

[21] H. Ruiz, N. Osawa and S. Rashed: A practical analysis of residual stresses induced by high-frequency mechanical impact post-weld treatment, *Welding in the World*, Vol.63, pp.1255–1263, 2019.
[22] J. Schubnell, P. Pontner, R.C. Wimpory, M. Farajian and V. Schulze: The influence of work hardening and residual stresses on the fatigue behavior of high frequency mechanical impact treated surface layers, *International Journal of Fatigue*, Vol.134, 105450, 2020.